Periodico di Mineralogia (2014), 83, 1, 121-140 DOI: 10.2451/2014PM0007

PERIODICO di MINERALOGIA
established in 1930

An International Journal of
MINERALOGY, CRYSTALLOGRAPHY, GEOCHEMISTRY,
ORE DEPOSITS, PETROLOGY, VOLCANOLOGY
and applied topics on *Environment*, *Archeometry* and *Cultural Heritage*

Reliability of the structural data for calcite and dolomite extracted from X-ray powder diffraction by Rietveld refinement

Shanke Liu[1,*], He Li[2], and Jianming Liu[1]

[1]Division of Solid Mineral Resources
[2]State Key Laboratory of Lithospheric Evolution,Institute of Geology and Geophysics,
Chinese Academy of Sciences, No. 19, Beitucheng Western Road, Chaoyang District, Beijing, 100029,
People's Republic of China
[*]Corresponding author: *liushanke@mail.iggcas.ac.cn*

Abstract

In this study, diffraction data of calcite and dolomite were collected using a conventional Bragg–Brentano diffractometer, which is a convenient, low-cost, and highly popular in-house instrument, and their crystal structures were refined by the Rietveld method. The effects of different refinement models on the structural data for calcite and dolomite are discussed and assessed in detail by comparing the data with those in literature. Different refinement models affect bond lengths and atomic coordinates of calcite and dolomite, whereas cell parameters are nearly unchanged. The results indicate the feasibility of extracting structural data of good quality from a conventional Bragg-Brentano diffractometer when appropriate strategies are applied.

Key words: calcite; dolomite; crystal structure; refinement strategy; preferred orientation.

Introduction

X-ray powder diffraction (XRPD) is a conventional method used for phase identification and quantitative analysis. Significant progress in powder methods occurred in the 1970s after Hugo Rietveld introduced a powerful technique for refining crystal structures from powder data in 1967. To evaluate the errors related to the practical application of the Rietveld method, the Commission on Powder Diffraction of the International Union of Crystallography performed

an intercomparison of the Rietveld refinements performed on two samples, namely, $PbSO_4$ and ZrO_2, using powder diffraction via a round-robin approach (Hill, 1992; Hill and Cranswick, 1994). Compared with single–crystal data, the light O atomic parameters from XRPD exhibit a wider distribution. However, a number of researchers (Grey et al., 1998; Ballirano, 2003) concluded that XRPD data can provide accurate results for the parameters related to oxygen when additional caution is taken during data collection and refinement procedures.

Ballirano (2011a) and Zucchini et al. (2012) compared single–crystal X–ray diffraction (SC–XRD) and XRPD data for calcite and dolomite obtained via Rietveld refinement. In particular, Ballirano (2011a) compared the XRPD data for calcite with those of SC–XRD analysis and proved the feasibility of extracting high-quality structural data using the former method. He also reported higher-quality in-house data relative to those from synchrotron X-ray powder diffraction (SN–XRPD) experiments. This finding was attributed to the use of an extended range of the analysed $\sin\theta/\lambda$ as compared to reference SN–XRPD (Antao et al., 2009). However, Ballirano (2011a) used a parallel-beam transmission X-ray powder diffraction (PT–XRPD), which is a different experimental set-up as compared to the conventional Bragg–Brentano one (BB–XRPD). Based on a comparison between BB–XRPD and SC–XRD data, Zucchini et al. (2012) reported that most of the crystal structural parameters of dolomite obtained from XRPD compare favourably with those obtained from SC–XRD. In their experiments, a number of parameters from XRPD were shown to be more accurate than those from SC–XRD, whereas others were less accurate. Hence, the methods complemented each other. Zucchini et al. (2012) also proposed that the preferred orientation effects contribute to the significantly biased results for powder samples.

Both calcite and dolomite exhibit rhombohedral cleavage, and, accordingly, their powders suffer for relevant preferred orientation whenever prepared as a front-loading flat-plate sample. For the transmission geometry, the most common cylindrical sample holder is the glass capillary. However, the popularity of the capillary is limited because of the disadvantages of this holder type (Cockcroft and Fitch, 2008) and the relative difficulties occurring during preparation and alignment of the sample. Nevertheless, a major advantage of the transmission geometry is that although samples may still exhibit a preferred orientation, such as when needle-shaped crystallites align with the horizontally rotated capillaries, the phenomenon has minimal effects on the results (McCusker et al., 1999; Cockcroft and Fitch, 2008). Regardless of the sample holder used, the studies of Ballirano (2011a) and Zucchini et al. (2012) both proved that high-quality structural data may be extracted from XRPD via the Rietveld method. The primary aim of both works by Ballirano (2011a) and Zucchini et al. (2012) was not to investigate the factors affecting the extraction of high–quality structural data from XRPD. These researchers simply modelled the preferred orientation using the spherical harmonics function (SPH) and did not extensively discuss the extent of the preferred orientation effects on

the structural parameters of calcite and dolomite. Thus, details regarding the effects of preferred orientation on the crystal structural data for calcite and dolomite are lacking.

In this study, the factors affecting the extraction of good quality structural data for calcite and dolomite via BB-XRPD combined with the Rietveld method were investigated. In particular, the effects of preferred orientation are discussed in detail. Although high-quality structural data are not easily extracted from BB-XRPD, the potential of this method, particularly in analysing natural mineral samples, was still explored because of its low cost and popularity.

Samples and measurement

Samples

As this study was aimed at evaluating the potential of the Rietveld method, no efforts for purifying natural mineral samples were performed. Two calcite samples were used: one (Mishan) was from Mishan, Heilongjiang Province, China, and the other (Occ) was from Rock-Mineral Preparation and Analysis Lab at the Institute of Geology and Geophysics, Chinese Academy of Sciences (IGGCAS). Two dolomite samples (LJM-1 and LJM-2) were mined from different sites in Chifeng, Inner Mongolia, China. To determine the chemical compositions of the two dolomite samples, a mixture of each powder sample (0.5 g) and $Li_2B_4O_7 + LiBO_2$ (5 g) was heated and fused into a glass disc. The composition of the mixture was then analysed by X-ray fluorescence spectroscopy (XRF) using a Shimadzu XRF 1500 sequential spectrometer (Shimadzu Corporation, Japan) at IGGCAS.

Acquisition of XRPD patterns

Each sample was uniformly ground using a mortar and pestle and passed through a 200-mesh sieve. Step-scanned patterns were acquired using a Rigaku Dmax 2400 Bragg-Brentano rotating-anode diffractometer fitted with a diffracted-beam graphite monochromator (Rigaku Corporation, Japan). Given that calcite and dolomite strongly prefer a specific orientation, samples were prepared by the back-loading method to reduce the effects of the preferred orientation. For the LJM-2 dolomite sample, parallel data (LJM-2p) were collected under different measurement conditions. Experimental details are listed in Table 1. Three of the samples, namely, LJM-1, LJM-2, and Mishan, contain impurities that were quantified as a part of the Rietveld refinements.

Rietveld refinement

The Rietveld method, which was initially proposed by Hugo Rietveld (1967, 1969), has been significantly improved during the last two decades and has become an effective, reliable tool for the structural analysis of various compounds with three-dimensional architecture.

The computer program package General Structure Analysis System (GSAS) (Larson and Von Dreele, 2000) and its graphical interface EXPGUI (Toby, 2001), which are freely available, were used for the structural refinements. The quality of fit for the experimental and calculated profiles obtained by

Table 1. XRPD data collection conditions.

Instrument	Rigaku Dmax 2400
Radiation	Cu rotating-anode tube, operated at 40 kV and 100 mA
Optics	Divergence slit = 1°, Scatter slit = 1°, Receiving slit = 0.15 mm
Sample holder	Rectangular aluminum plates with rectangular window
Monochromator	Graphite diffracted beam
Detector	NaI scintillator
Angular range (°2θ)	15-140 for all samples except for Mishan calcite(3-140)
Step size (°2θ)	0.02
Counting time (s/ step−1)	2 for LJM-1 and LJM-2; 0.5 for LJM-2p, Mishan, and Occ

the programs was verified using the LaB_6 standard (SRM 660B, National Institute of Standards and Technology, USA) XRPD pattern. The instrumental parameter file was obtained from the XRPD pattern of the LaB_6 standard.

Starting atomic coordinates, cell parameters, and isotropic temperature factors, of calcite and dolomite were taken from Markgraf and Reeder (1985) and Reeder and Wenk (1983), respectively. The background was modeled using a 10-term Chebyshev polynomial. The reflection-peak profiles were matched using the CW profile function 3 in GSAS (Finger et al., 1994). A full-matrix, least-squares refinement with varying scale factors, background parameters, cell parameters, displacement corrections, atomic coordinates, and isotropic temperature parameters rapidly converged.

One March–Dollase vector is generally chosen during refinements. However, natural calcite specimens often exhibit a strong preferred orientation with a c-axis maximum (Wenk and Houtte, 2004) non-coincident with the *104* plane. In our experiment, this phenomenon was observed for both calcite and dolomite. Therefore, two refinements were performed using one March–Dollase preferential orientation plane (*104*, MD1) and two preferential orientations planes (*104* and *001*, MD2), respectively. Several researchers (Sitepu 2002; Sitepu et al., 2005; Balic-Zunic et al., 2011) have shown that SPH is superior to the March–Dollase function in terms of correcting the preferred orientation effects. As a result, SPH was used to correct the peak intensities, and 10 harmonic orders were selected (Sitepu et al., 2005). To favor convergence toward a meaningful solution, a soft distance constraint (SDC) between the C and O atoms was further applied for all data except for those for Occ after SPH was used to correct the peak intensities. The constrained value between the C and O atoms was set to 1.285(10) Å.

Table 2. Chemical composition of dolomite samples (wt.%).

Sample	SiO_2	TiO_2	Al_2O_3	*TFe_2O_3	MnO	MgO	CaO	Na_2O	K_2O	P_2O_5	LOI	TOTAL
LJM-1	0.53	0.01	0.14	0.37	0.02	22.06	30.77	0.03	0.03	0.01	46.72	100.69
LJM-2	2.64	0.01	0.06	0.18	0.01	21.77	30.09	0.02	0.01	0.03	45.92	100.74

*T= total Fe as Fe_2O_3

Results and discussion

The chemical compositions of the dolomite samples are presented in Table 2. Except for Occ, all other samples contain few impurities that do not exceed 4 wt.%. Although dolomite samples are not pure, the dolomite phase content in each sample exceeds 96 wt.% based on the Rietveld quantitative phase analysis (QPA) (Table 3).

In this study, for the sake of simplicity the Ca/Mg ratio of dolomite was set to one. The fit did not improve when the site occupancies for Ca and Mg was allowed to refine. For the impurity phases, only the cell and profile parameters were refined. Refined structural parameters of calcite and dolomite are listed in Tables 4 and 5, respectively, whereas reference structural parameters of calcite and dolomite are reported in Table 6 for comparison purposes. The Rietveld plots of Mishan-SPH and LJM-1-SPH are shown as examples in Figures 1 and 2, respectively. Cell parameters of calcite and dolomite were plotted against the different refinement models in Figures 3 and 4, respectively. The selected bond lengths in calcite and in dolomite, and the atomic coordinates in dolomite were plotted against the different refinement models in Figures 5, 6, and 7, respectively. In Table 7, the parameter σ_D is presented for the quantificational assessment of the effects of the four different refinement models on the structural parameters of calcite and dolomite. The assessment was performed as follows, the *a* cell parameter of Mishan being used as an example: the difference Δ between the largest and the smallest value for the a cell parameter from the four different refinement

Table 3. Quantitative phase analyses of the various samples (wt.%).

	Dolomite	Calcite	Quartz	Albite	Microcline	Clinochlore
Mishan	/	98.21(1)	0.40(3)	/	/	1.39(5)
Occ	/	100.00(/)		/	/	/
LJM-1	98.24(1)2	0.51(3)	0.29(2)	0.50(6)	0.47(4)	/
LJM-2	96.63(2)	0.58(3)	2.38(4)	0.41(4)	/	/
LJM-2p	97.20(2)	0.40(3)	1.98(4)	0.42(5)	/	/

Note: 1. LJM-2p denotes that the repeated experiment was conducted using a different measurement condition.
2. Standard deviations are given in parentheses.

Table 4. Details of the refined crystal structure parameters of the calcite samples. Agreement indices as defined in Young (1993).

		Mishan			Occ				
		MD1	MD2	SPH	SDC	MD1	MD2	SPH	SDC
Cell Parameters	a/Å	4.9875(1)	4.9874(1)	4.9873(1)	4.9873(1)	4.9863(2)	4.9864(2)	4.9866(2)	/
	c/Å	17.0527(5)	17.0528(4)	17.0525(4)	17.0525(4)	17.0799(8)	17.0801(7)	17.0816(7)	/
	V/Å^3	367.35(2)	367.34(2)	367.33(2)	367.33(2)	367.77(4)	367.79(4)	367.84(4)	/
Atom Site	x_O	0.2487(4)	0.2523(3)	0.2535(5)	0.2560(2)	0.2542(3)	0.2548(3)	0.2572(5)	/
B_{iso}	Ca	1.22(3)	1.08(3)	1.13(3)	1.12(3)	0.97(2)	1.05(2)	1.03(3)	/
	C	1.21(3)	1.07(3)	1.12(3)	1.11(3)	0.96(2)	1.04(2)	1.02(3)	/
	O	1.79(3)	1.65(3)	1.65(3)	1.69(3)	1.54(2)	1.62(2)	1.60(3)	/
Bong Length	Ca-O	2.380(1)	2.370(1)	2.367(1)	2.3607(6)	2.3663(9)	2.3648(8)	2.359(1)	/
	C-O	1.240(2)	1.259(2)	1.264(3)	1.2766(12)	1.268(1)	1.271(1)	1.283(3)	/
R Factors	R_{WP}	16.5	15.0	14.1	14.1	14.4	12.9	12.6	/
	R_P	11.9	10.8	10.0	10.0	10.4	9.03	8.58	/
	Rexp	9.81	9.83	9.78	9.71	10.79	10.79	10.80	/
	R_{F2}	17.5	13.9	12.0	12.2	10.5	6.76	4.76	/
	χ^2	2.83	2.33	2.08	2.11	1.78	1.43	1.36	/
W_{SDC}		/	/	/	0.96	/	/	/	/
Texture index		/	/	2.06	2.11	/	/	1.41	/

Note: 1. MD1 denotes that only the preferred parameters of the *104* plane are refined through the March-Dollase model. MD2 denotes that the preferred parameters of *104* and *001* planes are both refined through the March-Dollase model. SPH denotes that the spherical harmonics function is introduced into the structural model to correct for preferred orientation. SDC denotes that a soft distance constraint for C-O bond length was imposed to the refinement.
2. Standard deviations are given in parentheses.

models. Afterward, the mean value of the four ESDs of the a cell parameter was calculated using the formula. Finally, σ_D was obtained using the formula $\sigma_D = \Delta/\sigma$.

Rietveld refinement of the calcite and dolomite crystal structures

R factors. The trend of the variation of the *R* factors when different refinement techniques are applied are similar for both calcite and dolomite samples (Tables 4 and 5). Except for R_{exp}, all *R* factors significantly decrease when MD2 and SPH, rather than MD1, are introduced to model the preferred orientations. Therefore, the textures for calcite and dolomite cannot be satisfactorily described by a single March-Dollase vector. However, the variations of the *R* factors for the calcite samples slightly differ from those of the dolomite samples when the refinement model is changed from MD2 to SPH. The *R* factors of Mishan and Occ decrease, whereas those of

Table 5. Details of the refined crystal structure parameters of the dolomite samples. Agreement indices as defined in Young (1993).

		LJM-1				LJM-2				LJM-2p			
		MD1	MD2	SPH	SDC	MD1	MD2	SPH	SDC	MD1	MD2	SPH	SDC
Cell Parameters	a/Å	4.8115(2)	4.8106(1)	4.8110(1)	4.8107(1)	4.8099(2)	4.8101(1)	4.8103(1)	4.8104(1)	4.8103(2)	4.8107(1)	4.8107(1)	4.8108(1)
	c/Å	16.0258(6)	16.0249(4)	16.0264(4)	16.0252(5)	16.0235(7)	16.0237(4)	16.0234(4)	16.0234(5)	16.0226(6)	16.0228(4)	16.0227(5)	16.0229(5)
	V/Å^3	321.29(3)	321.16(2)	321.25(2)	321.18(2)	321.05(3)	321.08(2)	321.09(2)	321.10(2)	321.08(3)	321.14(2)	321.13(2)	321.14(2)
Atom Sites	z_C	0.2439(1)	0.24305 (7)	0.2435(1)	0.2424(1)	0.2440(1)	0.24334(7)	0.24308(8)	0.24310(9)	0.2433(1)	0.24268(9)	0.2424(1)	0.2424(1)
	x_O	0.2389(6)	0.2447(4)	0.2441(5)	0.2455(2)	0.2397(5)	0.2433(4)	0.2408(5)	0.2454(2)	0.2398(5)	0.2440(4)	0.2417(6)	0.2464(1)
	y_O	−0.0367(6)	−0.0327(4)	−0.0371(4)	−0.0382(2)	−0.0361(5)	−0.0330(4)	−0.0372(4)	−0.0366(2)	−0.0371(5)	−0.0349(4)	−0.0365(5)	-0.0367(1)
	z_O	0.2451(1)	0.24421(7)	0.2433(1)	0.2435(1)	0.2451(1)	0.24444(7)	0.24418(8)	0.24420(9)	0.2444(1)	0.24378(9)	0.2435(1)	0.2435(1)
B_{iso}	Ca	1.27(4)	0.76(2)	1.31(2)	1.29(2)	1.49(3)	0.92(2)	1.58(2)	1.62(2)	1.37(3)	0.98(2)	1.39(3)	1.42(3)
	Mg	1.14(4)	0.63(2)	1.19(2)	1.16(2)	1.36(3)	0.79(2)	1.45(2)	1.49(2)	1.24(3)	0.85(2)	1.26(3)	1.29(3)
	C	1.18(4)	0.67(2)	1.22(2)	1.20(2)	1.40(3)	0.83(2)	1.49(2)	1.53(2)	1.28(3)	0.89(2)	1.30(3)	1.33(3)
	O	1.47(4)	0.96(2)	1.52(2)	1.49(2)	1.69(3)	1.12 (2)	1.78(2)	1.82(2)	1.57(3)	1.18(2)	1.59(3)	1.62(3)
Bond Length	Ca-O	2.396(3)	2.385(1)	2.402(2)	2.398(1)	2.392(2)	2.386(1)	2.401(2)	2.389(1)	2.401(2)	2.394(1)	2.404(2)	2.394(1)
	Mg-O	2.114(3)	2.106(1)	2.082(2)	2.076(1)	2.115(2)	2.110(1)	2.099(1)	2.089(1)	2.104(2)	2.095(1)	2.092(2)	2.079(1)
	C-O	1.247(3)	1.263(1)	1.273(2)	1.2828(9)	1.249(2)	1.258(1)	1.257(2)	1.2778(9)	1.252(2)	1.266(1)	1.260(2)	1.2829(1)
R Factors	R_{WP}	19.1	11.7	11.8	11.8	17.1	11.2	11.5	11.9	19.7	13.4	14.0	14.09
	R_P	12.1	7.66	7.90	7391	11.3	7.96	7.91	8.03	11.9	8.68	8.91	9.00
	Rexp	3.73	3.85	3.75	3.75	3.65	3.65	3.64	3.62	8.53	8.08	8.08	8.07
	R_{F2}	20.6	8.13	8.76	8.90	17.7	7.79	8.09	8.47	17.4	7.24	7.73	7.77
	$\chi 2$	26.2	9.24	9.92	9.92	21.9	9.44	10.0	10.8	5.34	2.75	3.00	3.05
W_{SDC}		/	/	/	0.14	/	/	/	1.56	/	/	/	0.38
Texture index		/	/	4.46	4.57	/	/	4.53	4.85	/	/	3.23	3.39

Note: 1. MD1 denotes that only the preferred parameters of the *104* plane are refined through the March-Dollase model. MD2 denotes that the preferred parameters of *104* and *001* planes are both refined through the March-Dollase model. SPH denotes that the spherical harmonics function is introduced into the structural model to correct the preferred orientation. SDC denotes that a soft distance constraint for C-O bond length was imposed to the refinement.

2. Standard deviations are given in parentheses.

Table 6. Details of the reference structural parameters of calcite and dolomite.

		Calcite				Dolomite		
		Markgraf and Reeder (1985)	Antao et al. (2009)	Sitepu et al. (2005)*	Ballirano (2011a)*	Reeder and Wenk (1983)	Zucchini et al. (2012)*	
Cell Parameters	a/Å	4.988(1)	4.9877648(1)	4.9920(5)	4.98879(7)	4.8038(9)	4.8111(1)	4.80777(3)
	c/Å	17.061(1)	17.05242(2)	17.069(2)	17.0649(4)	16.006(4)	16.035(4)	16.0091(1)
	V/Å^3	367.6(1)	367.3911(4)	368.3731	367.81(1)	319.88(8)	321.4(1)	320.468(2)
Atom Sites	z_C	/	/	/	/	0.24266(5)	0.2429(1)	0.2461(4)
	x_O	0.2567(2)	0.25734(6)	0.250(1)	0.2564(9)	0.24762(9)	−0.2830(2)	0.2445(5)
	y_O	/	/	/	/	−0.03535(9)	−0.0355(2)	-0.0356(6)
	z_O	/	/	/	/	0.24406(2)	0.24400(2)	0.2435(2)
B_{iso}	Ca	0.94(3)	0.80(4)	1.203(4)	-	0.66(1)	0.77(3)	1.24(5)
	Mg	/	/	/	/	0.53(1)	0.64(4)	1.03(7)
	C	0.93(5)	0.76(6)	1.644(2)	-	0.57(1)	0.67(5)	0.50(9)
	O	1.51(4)	1.44(6)	1.644(2)	-	0.86(1)	0.95(3)	1.56(5)
Bond Length	Ca-O(3a)	2.3595(5)	2.3574(2)	2.379(1)	2.3608(7)	2.3802(6)	2.3852(4)	2.395(1)
	Mg-O(3b)	/	/	/	/	2.0839(5)	2.0864(4)	2.087(1)
	C-O	1.280(1)	1.2836(3)	1.248(2)	1.279(1)	1.2826(6)	1.2848(6)	1.270(1)
Method		SC-XRD	SN-XRPD	BB-XRPD	PT-XRPD	SC-XRD	SC-XRD	BB-XRPD

Note: *Bond lengths are calculated in terms of cell parameters and atomic coordinates in their studies. Standard deviations are given in parentheses.

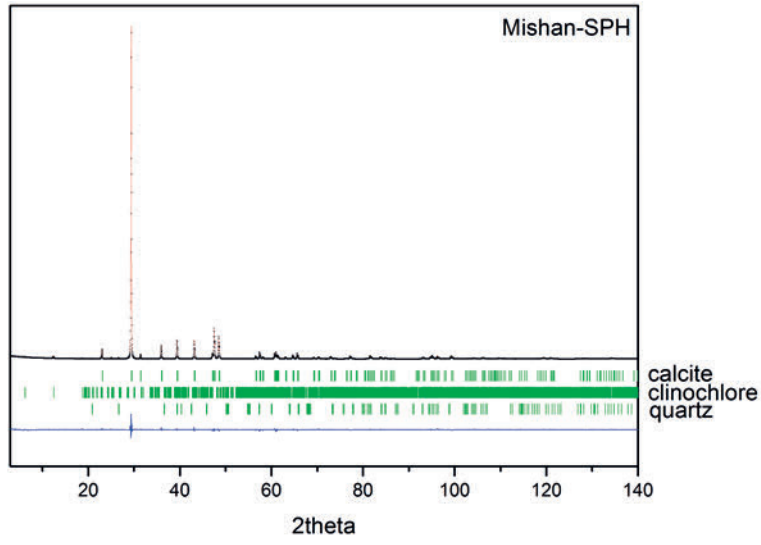

Figure 1. Rietveld fit of Mishan-SPH: the upper curves are observed (crosses) and calculated (line) diffraction patterns; vertical marks indicate the positions of allowed *Kα1* and *Kα2* reflections; the curve at the bottom shows the difference between observed and calculated patterns.

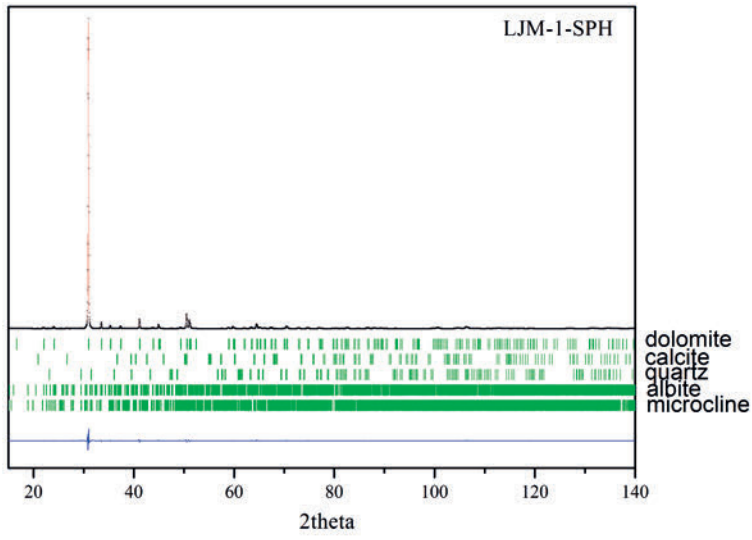

Figure 2. Rietveld fit of LJM-1-SPH: the upper curves are observed (crosses) and calculated(line) diffraction patterns; vertical marks indicate the positions of allowed *Kα1* and *Kα2* reflections; the curve at the bottom shows the difference between observed and calculated patterns.

LJM-1, LJM-2, and LJM-2p slightly increase. When SDC is applied, the *R* factors for the LJM-1, LJM-2, and Mishan samples slightly increase. Toby (2006) stated that agreement factors are not the only indicators of the quality of a Rietveld fit and the greater chemical plausibility allows us to state that model SDC is preferred.

Cell parameters. The cell parameters show negligible changes when different refinement models are applied, as clearly observed in Figures 3 and 4. The variations for the calcite samples are approximately ± 2σ, whereas those for LJM-1 (approximately ± 5σ) are larger than those for LJM-2 (approximately ± 3σ). The cell parameters refined by the different refinement models in this paper are primarily consistent with the literature values (Figure 3 for calcite and Figure 4 for dolomite). Figure 3 shows that the a and V cell parameters of Mishan and Occ approach those reported by Antao et al. (2009), Ballirano (2011a), and Markgraf and Reeder (1985). However, the a and V cell parameters reported by Sitepu et al. (2005) both deviate from the cell parameters obtained in this paper and from those reported in reference data. The c cell parameters in this paper and those reported in previous studies appear moderately scattered. The c cell parameters of Mishan and Occ in this paper approach the values obtained by Antao et al. (2009) and Sitepu et al. (2005), respectively. All the dolomite cell parameters in this paper are closer to the values obtained by Zucchini et al. (2012) from BB-XRPD data (Figure 4) but slightly deviate from the data reported in other studies (Reeder and Wenk, 1983; SC-XRD data

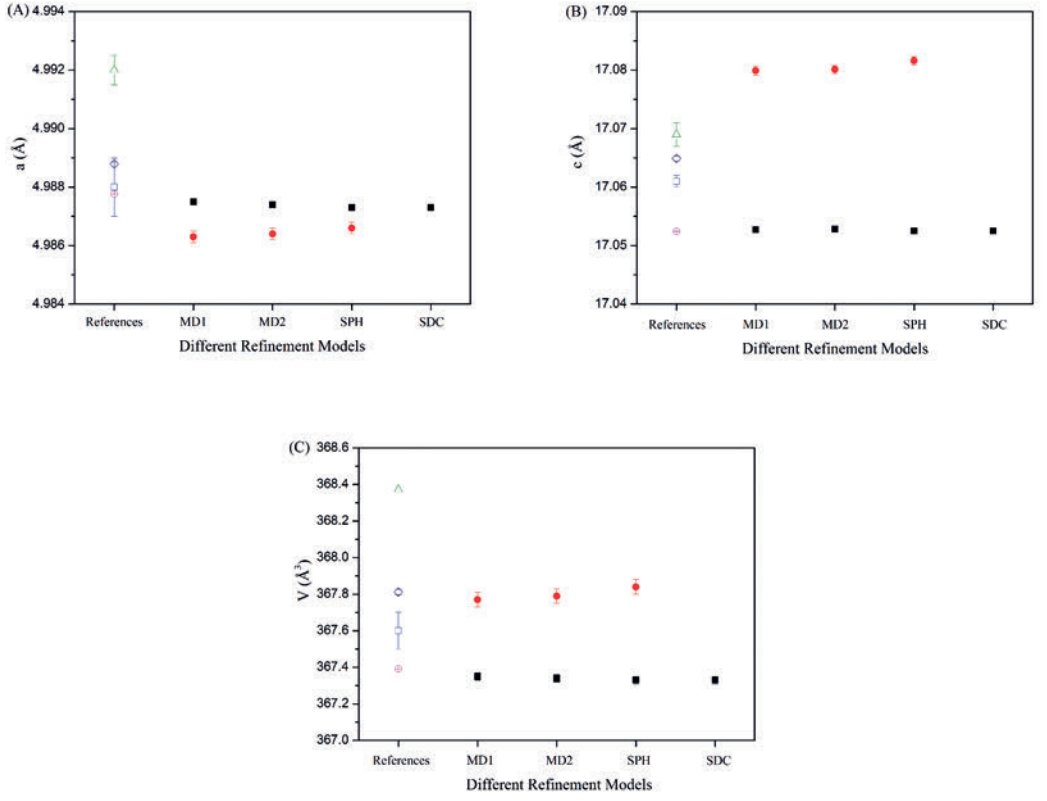

Figure 3. Cell parameters of calcite plotted against different refinement models (DRM): (A) *a* versus DRM; (B) *c* versus DRM; (C) *V* versus DRM. ■ Mishan; ● Occ; □ Markgraf and Reeder (1985); ○ Antao et al. (2009); △ Sitepu et al. (2005); ◇ Ballirano (2011a). The vertical bars represent errors. If no bar is given, then the error is contained within the area of the symbol.

of Zucchini et al., 2012). The parallel data for LJM-2p (filled triangles) nearly overlap with those of LJM-2 (filled circles). All the dolomite samples reported in other studies were obtained from a metamorphic carbonate complex in Eugui, Spain. However, the data for the Eugui dolomite samples appear to be moderately scattered, possibly because of the experimental errors committed by the different researchers, different chemical compositon and/or strain for the Eugui dolomite, as well as the varied methods used. Given that the corundum lattice parameters refined by the Rietveld method perfectly fit the theoretical values, Zucchini et al. (2012) confirmed the feasibility of determining cell parameters via Rietveld refinement of BB-XRPD data.

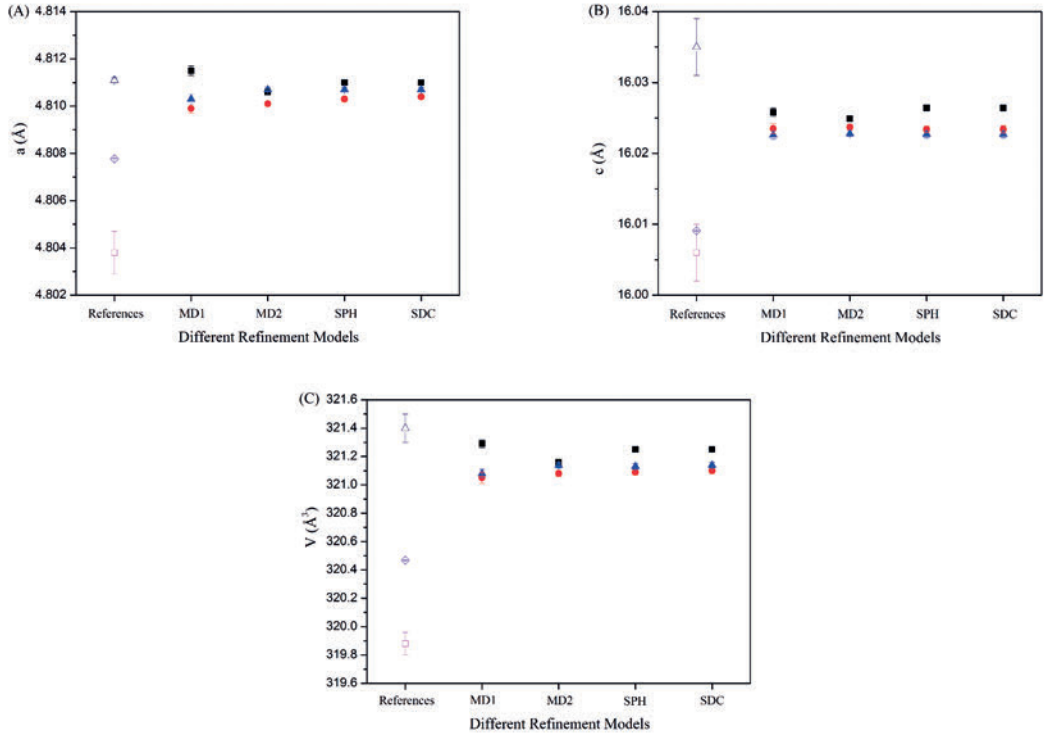

Figure 4. Cell parameters of dolomite plotted against different refinement models (DRM): (A) *a* versus DRM; (B) *c* versus DRM; (C) *V* versus DRM. ■ LJM-1; ● LJM-2; ▲ LJM-2p; □ Reeder and Wenk (1983); △ Zucchini et al. (2012) SC-XRD; ◇ Zucchini et al. (2012) BB-XRPD. The vertical bars represent errors. If no bar is given, then the error is contained within the area of the symbol.

Isotropic displacement factors. The different refinement models show negligible effects on the isotropic displacement factors (Bisos) of calcite. However, the effects of these models on the Bisos of dolomite vary. The Bisos of dolomite remains nearly unchanged upon use of the various preferred orientation corrections MD1, SPH, and SDC but clearly decreases when MD2 is used to correct the peak intensities. When *104* and *001* are introduced as preferential orientations, the preferred fractions are approximately 20% and 80%, respectively. The *001* diffraction peaks for the dolomite samples are possibly overcorrected by the March–Dollase function and thus results in a clearly reduced Bisos. Table 6 shows that for both calcite and dolomite, the Bisos obtained from BB-XRPD data (Sitepu et al., 2005; Zucchini et al., 2012) are greater than those from SC-XRD (Markgraf and Reeder, 1985; Reeder and Wenk, 1983; Zucchini et al., 2012). However, the Bisos of the atoms in calcite reported by Sitepu et al. (2005) and the Bisos of the atoms in

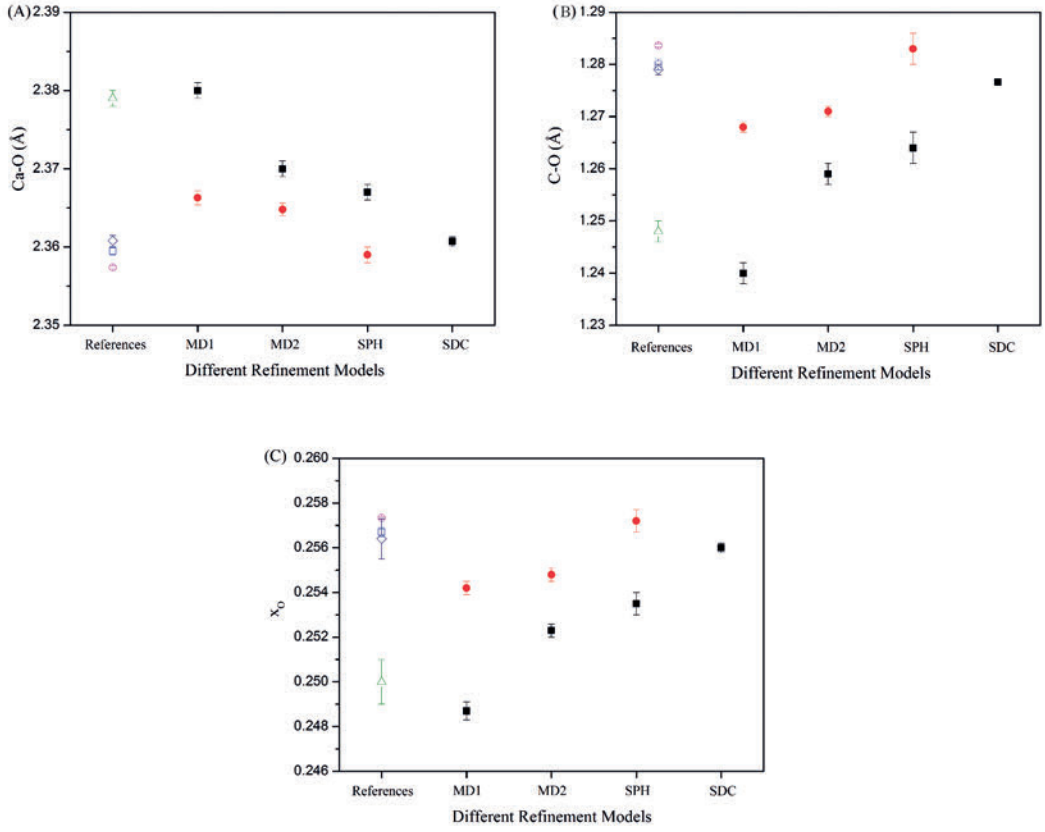

Figure 5. Bond lengths of calcite plotted against different refinement models (DRM): (A) Ca-O versus DRM; (B) C-O versus DRM; (C) x_O versus DRM. ■ Mishan; ● Occ; □ Markgraf and Reeder (1985); ○ Antao et al. (2009); △ Sitepu et al. (2005); ◇ Ballirano (2011a). The vertical bars represent errors. If no bar is given, then the error is contained within the area of the symbol.

dolomite obtained by Zucchini et al. (BB-XRPD, 2012) are consistent with the Bisos obtained in this paper, except for those of the C atoms. The difference between the Biso of the C atom in this paper and that in literature (Sitepu et al., 2005; BB-XRPD, Zucchini et al., 2012) may be due to the different refinement strategies. Sitepu et al. (2005) assumed that the Biso of the C atom was equal to that of an O atom, whereas Zucchini et al. (2012) did not constrain the Biso of the C atom during the refinement. However, we found that the Biso of the C atom significantly decreases when no constraints are introduced during the refinement. To prevent the C atom Biso from becoming too small, the same multipliers were used for the Bisos of the C and O atoms during the refinement.

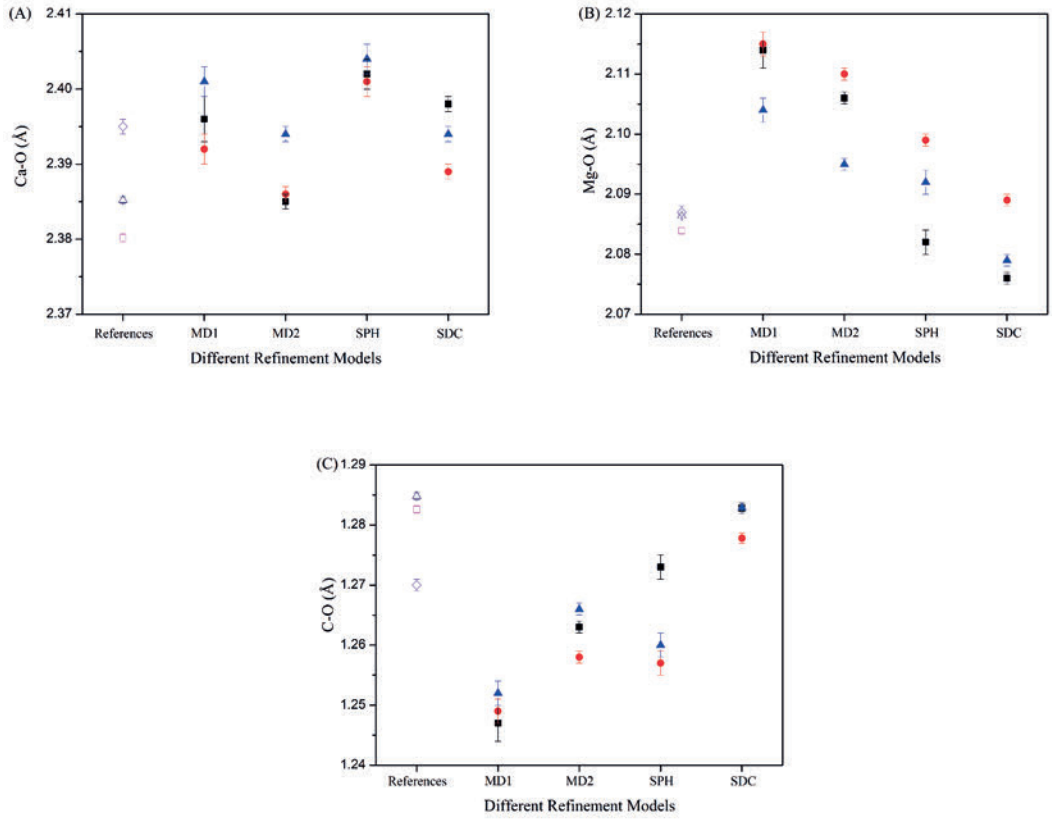

Figure 6. Selected bond lengths of dolomite plotted against different refinement models (DRM): (A) Ca-O versus DRM; (B) Mg-O versus DRM; (C) C-O versus DRM. ■ LJM-1; ● LJM-2; ▲ LJM-2p; □ Reeder and Wenk (1983); △ Zucchini et al. (2012) SC-XRD; ◇ Zucchini et al. (2012) BB-XPRD. The vertical bars represent errors. If no bar is given, then the error is contained within the area of the symbol.

Bond lengths and atomic coordinates. Figure 5(A) and (B) shows that the refinement models exhibit opposite effects on the Ca–O and C–O bond lengths. In calcite, the calcium layers and planar CO_3^{2-} groups alternate along the c axis, and calcium is in octahedral coordination with six oxygen ions from six different carbonate groups. Only the x_O in calcite can vary in the structural model; the other coordinates are fixed during the refinement because of their special positions. Due to this fact, the Ca–O bond length decreases as the C–O bond length increases. The Ca–O and C–O bond lengths are anticorrelated because of the variations in the oxygen atomic coordinates with different refinement models. The σ_Ds of the bond lengths for Mishan and Occ are approximately ± 19σ and ± 8σ, respectively, and the σ_Ds of the bond lengths are nearly the

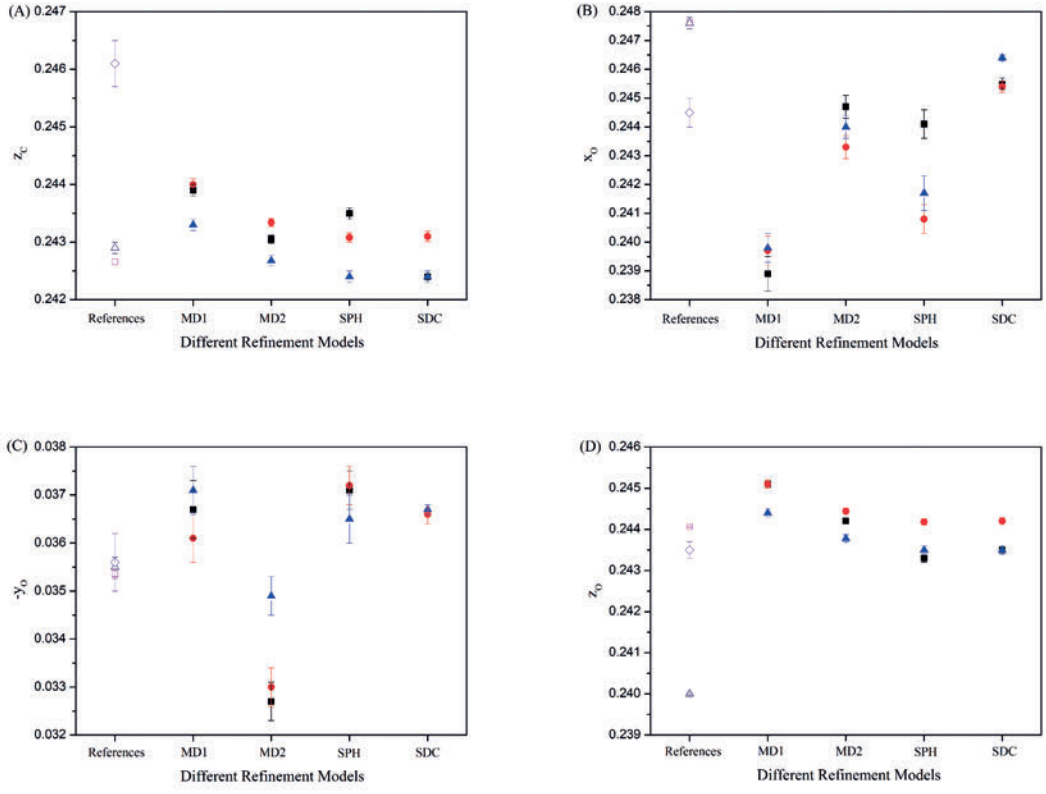

Figure 7. Atomic coordinates of dolomite plotted against different refinement models (DRM): (A) z_C versus DRM; (B) x_O versus DRM; (C) y_O versus DRM; (D) z_O versus DRM ■ LJM-1; ● LJM-2; ▲ LJM-2p; □ Reeder and Wenk (1983); △ Zucchini et al. (2012) SC-XRD; ◇ Zucchini et al. (2012) BB-XPRD. The vertical bars represent errors. If no bar is given, then the error is contained within the area of the symbol.

same as the respective σ_Ds of x_O. Therefore, the effects of the different refinement models on Mishan are greater than those on Occ. In fact, σ_Ds of the bond lenths and x_O are closely related to the texture of the sample. More heavier correction for preferred orientation, and more change for structural parameters. As a result, σ_Ds become larger. For both calcite samples, the Ca–O and C–O bond lengths deviate from those reported by Antao et al. (2009), Ballirano (2011a), and Markgraf and Reeder (1985) when MD1 and MD2 are introduced to model the preferred orientations (Figure 5). The Ca–O (2.36 Å) and C–O (1.28 Å) bond lengths of Occ are highly consistent with those obtained by Antao et al. (2009), Ballirano (2011a), and

Table 7. σ_D of the structure parameters of calcite and dolomite among different refinement methods.

	Mishan	Occ	LJM-1	LJM-2	LJM-2p
a	2	2	7	4	4
c	1	2	3	1	1
V	1	2	6	2	3
Ca-O	21	8	9	10	6
Mg-O	/	/	19	24	17
C-O	17	8	19	18	21
z_C	/	/	16	11	9
x_O	20	8	15	14	15
y_O	/	/	13	11	5
z_O	/	/	19	11	9

Markgraf and Reeder (1985). However, the values for Mishan (Ca–O = 2.37 Å; C–O = 1.26Å) slightly deviate from the reference values (Antao et al., 2009; Ballirano, 2011a; Markgraf and Reeder, 1985) when SPH is introduced (Figure 5). For Mishan, the Ca–O and C–O bond lengths are in good agreement with those reported by Antao et al. (2009), Ballirano (2011a), and Markgraf and Reeder (1985) only when SDC is further applied (Figure 5). For both Occ and Mishan, the bond lengths approach the published values when SPH is introduced into the structural model (Figure 5).

In dolomite, the z_C, x_O, y_O, and z_O vary in the structural model, whereas the remaining coordinates are in special position. The variations of the bond lengths and atomic coordinates of dolomite with the refinement models is more complex than those of calcite (Figures 6 and 7 and Tables 5-7). The variations of the Ca–O bond lengths of the dolomite samples are smaller than those of the Mg–O and C–O bond lengths. The σ_D of the Ca–O bond lengths of the dolomite samples is less than ± 10σ, whereas the σ_Ds of the Mg–O and C–O bond lengths of the dolomite samples are approximately ± 20σ and ± 19σ, respectively (Table 7). This finding indicates that the effects of the different refinement models on the Ca–O bond lengths of the dolomite samples are smaller than those on the Mg–O and C–O bond lengths. Besides, the Mg–O and C–O bond lengths of these dolomite samples are anticorrelated. Similarly, σ_Ds are closely related to the texture. The Ca–O bond lengths of the dolomite samples, which slightly deviate from those refined from SC-XRD data by Reeder and Wenk (1983) and Zucchini et al. (2012), fluctuate around those refined from the BB-XRPD data by Zucchini et al. (2012) when the four different models are applied. The Mg–O bond lengths of the dolomite samples are consistent with the published values (SC-XRD of Reeder and Wenk, 1983; SC-XRD and BB-XRPD of Zucchini et al., 2012) when SPH and SDC are applied, but their Mg–O bond lengths slightly deviate from the published

values when MD1 and MD2 are applied. When SPH is applied, the C–O bond length of the LJM-1 sample is approximately 1.27 Å, which approaches the value obtained by Zucchini et al. (BB-XRPD, 2012). The C–O bond length of the LJM-1 sample with the SPH model is longer than those obtained using the MD1 and MD2 models. The C–O bond lengths (approximately 1.26 Å) of the LJM-2 sample refined using the SPH and MD2 models are highly similar. Moreover, these values are smaller than those obtained by Zucchini et al. (2012, BB-XRPD) but larger than those obtained using the MD1 model. The C–O bond lengths of the LJM-1 and LJM-2 samples after refinement with the SDC model are approximately 1.28 Å and are consistent with the SC-XRD values obtained by Reeder and Wenk (1983) and Zucchini et al. (2012).

Reliability of the structural data for calcite and dolomite extracted from BB-XRPD

Preferred orientation corrections are strongly correlated with the bond lengths as they modify the observed structural factor and thus affect the atomic coordinates. The bond lengths of calcite are consistent with the values obtained from the refinement of SC-XRD (Markgraf and Reeder, 1985), SN-XRPD (Antao et al., 2009), and PT-XRPD (Ballirano, 2011a) data when the appropriate model (the SPH model for Occ; the SDC model for Mishan) is used. Although the variations in the bond lengths of dolomite appear more complex when different refinement models are used, the bond lengths of dolomite in this paper are consistent with those obtained from SC-XRD data (Reeder and Wenk, 1983; Zucchini et al., 2012) when SDC is introduced into the structural model. In the carbonates, the C–O bond length is 1.28 Å to 1.29 Å based on SC-XRD (Effenberger et al., 1981; Markgraf and Reeder, 1985; Reeder and Wenk, 1983; Zucchini et al., 2012), SN-XRPD (Antao et al., 2009), and PT-XRPD (Ballirano, 2011a) data. In this study, the C–O bond lengths of the Mishan, LJM-1, and LJM-2 samples as well as those obtained from BB-XRPD in literature (Sitepu et al., 2005; Zucchini et al., 2012) are 0.01 Å to 0.03 Å shorter than the 1.28 Å obtained when SPH is used to correct the peak intensities. However, another point must be considered when assessing the precision of a bond distance. The mean square amplitude of the vibration of the atoms in calcite and dolomite is approximately 0.01 $Å^2$. This result indicates that the mean amplitude of vibration is approximately 0.1 Å. In general, people often forget that atoms are constantly moving and are thus misled by the pictures and models used to visualize crystal structures. Therefore, the meaning of measuring a bond distance to the precision of 0.01 Å must also be considered when the atoms vibrate by ten times that amplitude (Kaduk, 1997).

Imposing of SDC improves the accuracy of the structural data for both calcite and dolomite. Using the calcite sample Mishan as an example, the absolute differences between the Ca–O and C–O bond lengths in this paper and those reported in literature (Markgraf and Reeder, 1985) are approximately 0.007 and 0.016Å, respectively, when SPH is introduced into the refinement model. However, the absolute

differences are approximately 0.001 and 0.003 Å, respectively, when SDC is introduced into the refinement model. For the dolomite samples, with LJM-1as an example, the absolute differences between the Ca–O, Mg–O, and C–O bond lengths in this paper and those reported in literature (Reeder and Wenk, 1983) are 0.022, 0.002, and 0.010 Å, respectively, when SPH is introduced into the refinement model. However, these values are approximately 0.018, 0.008, and 0.0002Å, respectively, when SDC is introduced into the model. The average absolute difference between the bond lengths in this paper and those published in literature (Reeder and Wenk, 1983) decreases from 0.011 Å to 0.009 Å when the refinement model is changed from SPH to SDC. The absolute differences between the z_C, x_O, y_O, and z_O in this paper and those reported in literature (Reeder and Wenk, 1983) are 0.0008, 0.0035, 0.0018, and 0.0008, respectively, when SPH is introduced into the refinement model; however, these values change to 0.0003, 0.0021, 0.0029, and 0.0006, respectively, when SDC is introduced. The average absolute difference of the coordinate values in this paper and those published in literature (Reeder and Wenk, 1983) decreases from 0.0017 to 0.0014 when the refinement model is changed from SPH to SDC. Therefore, the bond lengths and atomic coordinates of the LJM-1 dolomite approach the published values (Reeder and Wenk, 1983) when SDC is introduced into the structural model. In this study, similar trends are observed when the bond lengths and atomic coordinates are compared with those reported by Zucchini et al. (SC-XRD data, 2012). A number of researchers have investigated the structure of kaolinite using conventional BB-XRPD (Bish and Von Dreele, 1989; Suitch and Young, 1983) and neutron X-ray diffraction (Adams, 1983; Akiba et al., 1997; Bish, 1993; Suitch and Young, 1983; Young and Hewat, 1988). Accordingly, the distance between Al/Si–O obtained from the XRPD showed wider distribution than expected (Akiba et al., 1997; Smrcok, 1995; Suitch and Young, 1983; Young and Hewat, 1988). Therefore, the researchers had to refine the kaolinite structure using the soft distance constraint (Akiba et al., 1997; Bish, 1993; Bish and Von Dreele, 1989) to improve the accuracy of the structural data. The results have proven the effectiveness of soft distance constraint application. In this paper, the relative contribution (W_{SDC}) of the soft distance constraint to the total χ^2 in the final stages of refinement is less than 2.0% for the calcite and dolomite samples (Tables 4 and 5). Taking Mishan as an example, the restraint weight is 50 in Table 4 when SDC is applied. When the restraint weight is increased, the C-O bond length approaches the restrained value, and the Ca-O bond length and x_O sites are also changed. However, other parameters are nearly unchanged. Although it is almost a rigid-body refinement for SDC, the authors prefer SDC model according to a chemical plausibility, especially for a well known calcite structure that has been successfully refined many times (Antao et al., 2009; Ballirano, 2011a; Markgraf and Reeder, 1985).

In the introduction, we stated that a number of authors (Grey et al., 1998; Ballirano, 2003, 2011a, 2011b) have proven that XRPD data can

provide accurate results for the parameters related to oxygen when extra caution is taken during data collection and refinement procedures. Of these authors, Ballirano (2011a) performed a parallel-beam transmission using a position-sensitive detector and extracted high-quality data for calcite from XRPD. A transmission diffraction geometry was used in Ballirano's experiment, whereas reflection geometry was used in this paper. The Occ structural data obtained using the SPH model are highly consistent with the published values (Markgraf and Reeder, 1985; Antao et al., 2009; Ballirano, 2011a). The current results and Balliarno's (2011a) findings prove that high-quality data for calcite can be extracted from both transmission and reflection geometries. The texture index of Occ is 1.41, and the preferred orientation is not severe. Therefore, the texture of Occ is accurately described by SPH. In Ballirano's experiment, the preferred orientation was almost completely removed by the transmission geometry. We believe that the high-quality structural data for calcite in this paper and in Ballirano's study benefit from the high-quality diffraction data, which show less severe preferential orientation. The other samples in this study exhibit strong preference for specific orientations because of the extremely large texture indices of these samples. This strong preferred orientation significantly affects the diffraction data. For calcite and dolomite, *104* diffraction peak is the strongest one, and the preferred orientation further magnificate its intensity. In the Rietveld fits, the largest misfits are caused by the residuals of the *104* diffraction peak (Figures 1 and 2), which result in a sharp increase in the cumulative χ^2 plot. We also attempted to modify the structural model by refining the particle size components as well as the microstrain components. However, these refinements did not improve the fit. Thus, size and strain effects are not extensively discussed in this paper. In summary, we conclude that the preferred orientation is the principal factor that affects the quality of the BB-XRPD diffraction data for calcite and dolomite.

Conclusion

Calcite and dolomite structural data extracted from BB-XRPD using different refinement models were obtained, and the results were compared with published values. The following conclusions were drawn:

(1) High-quality structural data for calcite and dolomite can be extracted from BB-XRPD by the Rietveld method when the appropriate strategy is introduced into the structural model; the structural parameters are consistent with the published SC-XRD data (Markgraf and Reeder, 1985; Reeder and Wenk, 1983; Zucchini et al., 2012).

(2) The bond lengths and atomic coordinates of calcite and dolomite are significantly affected by the different refinement models; however, the cell parameters remain nearly unchanged.

(3) The Ca–O and C–O bond lengths in the calcite samples and the Mg–O and C–O bond lengths in the dolomite samples are anticorrelated. This condition is closely related to the structural geometry of the samples.

(4) The isotropic displacement factors obtained from BB-XRPD in this paper are larger than those obtained from SC-XRD (Markgraf and Reeder, 1985; Reeder and Wenk, 1983; Zucchini et al., 2012). However, these values are close to the published BB-XRPD results (Sitepu et al., 2005; Zucchini et al., 2012).

(5) Preferred orientation is the principal factor affecting the quality of the diffraction data for calcite and dolomite. As a result, the atomic coordinates and bond lengths deviate from their expected values.

Acknowledgments

The authors would like to acknowledge the financial support for technological innovations from the Institute of Geology and Geophysics, Chinese Academy of Sciences. Shanke Liu is indebted to Professor Jiaju Li for his tremendous help and encouragement in studying the Rietveld method. Shanke Liu is also grateful to Dr. B.H. Toby for helping him improve his GSAS refinement skills through private communications. Reviewer Prof. Paolo Ballirano and Editor Antonio Gianfagna are thanked for their constructive critical suggestions aimed to improve the quality of the manuscript.

References

Adams J.M. (1983) - Hydrogen atom positions in kaolinite by neutron profile refinement. *Clays and Clay Minerals*, 31(5), 352-356.

Akiba E., Hayakawa H., Hayashi S., Miyawaki R., Tomura, S., Shibasaki Y., Izumi F., Asano H. and Kamiyama T. (1997) - Structure refinement of synthetic deuterated kaolinite by Rietveld analysis using time-of-flight neutron powder diffraction data. *Clays and Clay Minerals*, 45(6), 781-788.

Antao S.M., Hassan I., Mulder W.H., Lee P.L. and Toby B.H. (2009) - In situ study of the R-3c→R-3m orientational disorder in calcite. *Physics and Chemistry of Minerals*, 36, 159-169.

Balic-Zunic T., Katerinopoulou A. and Edsberg A. (2011) - Application of powder X-ray diffraction and the Rietveld method to the analysis of oxidation processes and products in sulphidic mine tailings. *Neues Jahrbuch für Mineralogie*, 188(1), 31-47.

Ballirano P. (2003) - Effects of the choice of different ionization level for scattering curves and correction for small preferred orientation in Rietveld refinement: the $MgAl_2O_4$ test case. *Journal of Applied Crystallography*, 36, 1056-1061.

Ballirano P. (2011a) - Laboratory parallel-beam transmission X-ray powder diffraction investigation of the thermal behavior of calcite: comparison with X-ray single-crystal and synchrotron powder diffraction data. *Periodico di Mineralogia*, 80(1), 123-134.

Ballirano P. (2011b) - Laboratory parallel-beam transmission X-ray powder diffraction investigation of the thermal behavior of nitratine $NaNO_3$: spontaneous strain and structure evolution. *Physics and Chemistry of Minerals*, 38, 531-541.

Bish D.L. (1993) - Rietveld refinement of the kaolinite structure at 1.5k. *Clays and Clay Minerals*, 41(6), 738-744.

Bish D.L. and Von Dreele R.B.(1989) - Rietveld refinement of non-hydrogen atomic positions in kaolinite. *Clays and Clay Minerals*, 37(4), 289-296.

Cockcroft J.K. and Fitch A.N. (2008) - *Chapter 2 Experimental setups*: in Powder diffraction theory and practice (R.E. Dinnebier and S.J.L. Billinge ed.). RSC publishing, pp. 41.

Effenberger H., Mereiter K. and Zemann J. (1981) - Crystal structure refinements of magnesite, calcite, rhodochrosite, siderite, smithonite, and dolomite, with discussion of some aspects of the stereochemistry of calcite type carbonates. *Zeitschrift für Kristallographie*, 156, 233-243.

Finger L.W., Cox D.E. and Jephcoat A.P. (1994) - A correction for powder diffraction peak asymmetry due to axial divergence. *Journal of Applied Crystallography*, 27, 892-900.

Grey I.E., Cranswick L.M.D. and Li C. (1998) - Accurate site occupancies for light atoms from

powder X-ray data? Oxygen/vacancy ordering in 6H-$BaFe_{0.67}Ti_{0.33}O_{3-\delta}$ (δ = 0.08 and 0.32). *Journal of Applied Crystallography*, 31, 692-699.

Hill R.J. (1992) - Rietveld refinement round robin.I. Analysis of standard X-ray and neutron data for $PbSO_4$. *Journal of Applied Crystallography*, 25, 589-610.

Hill R.J. and Cranswick L.M.D. (1994) - International union of crystallography commission on powder diffraction Rietveld refinement round robin.II. Analysis of monoclinic ZrO_2. *Journal of Applied Crystallography*, 27, 802-844.

Kaduk J.A. (1997) - Chemical accuracy and precision in structural refinements from powder diffraction data. *The International Centre for Diffraction Data*, 40, 352-370.

Larson A.C. and Von Dreele R.B. (2000) - General Structure Analysis System (GSAS). *Los Alamos National Laboratory Report*. LAUR, 86-748.

Markgraf S.A. and Reeder R.J. (1985) - High-temperature structure refinements of calcite and magnesite. *American Mineralogist*, 70, 590-600.

McCusker L.B., Von Dreele R.B., Cox D.E., Louër D. and Scardi P. (1999) - Rietveld refinement guidelines. *Journal of Applied Crystallography*, 32, 36-50.

Reeder R.J. and Wenk H.R. (1983) - Structure refinements of some thermally disordered dolomites. *American Mineralogist*, 68, 769-777.

Rietveld H. (1967) - Line profiles of neutron powder-diffraction peaks for structure refinement. *Acta Crystallographica*, 22, 151-152.

Rietveld H.(1969) - A profile refinement method for nuclear and magnetic structures. *Journal of Applied Crystallography*, 2, 65-71.

Sitepu H. (2002) - Assessment of preferred orientation with neutron powder diffraction data. *Journal of Applied Crystallography*, 35, 274-277.

Sitepu H., O'Connor B.H. and Li D.Y. (2005) - Comparative evaluation of the March and generalized spherical harmonic preferred orientation models using X-ray diffraction data for molybdite and calcite powders. *Journal of Applied Crystallography*, 38, 158-167.

Smrcok L. (1995) - A comparison of powder diffraction studies of kaolin group minerals. *Zeitschrift für Kristallographie*, 210, 177-183.

Suitch P.R. and Young R.A. (1983) - Atom positions in highly ordered kaolinite. *Clays and Clay Minerals*, 31(5), 357-366.

Toby B.H. (2001) - EXPGUI, a graphical user interface for GSAS. *Journal of Applied Crystallography*, 34, 210-213.

Toby B.H. (2006) - R factors in Rietveld analysis: How good is good enough? *Powder Diffraction*, 21(1), 67-70.

Wenk H.R. and Houtte P.V. (2004) - Texture and anisotropy. *Reports on Progress in Physics*, 67, 1367-1428.

Young R.A. and Hewat A.W. (1988) - Verification of the triclinic crystal structure of kaolinite. *Clays and Clay Minerals*, 36(3), 225-232.

Zucchini A., Comodi P.,Katerinopoulou A., Balic-Zunic T., McCammon, C. and Frondini, F. (2012) - Order–disorder–reorder process in thermally treated dolomite samples: a combined powder and single-crystal X-ray diffraction study. *Physics and Chemistry of Minerals*, 39, 319-328.

Young R.A. (1993) - *Introduction to the Rietveld method*: In The Rietveld method (R.A. Young ed.). Oxford University Press, 1-38.

Submitted, January 2014 - Accepted, March 2014